

## Effect of Organic Modification on Structure and Properties of Room-Temperature Vulcanized Silicone Rubber/Montmorillonite Nanocomposites

Wang Jincheng, Hao Wenli

Department of Polymeric Materials and Engineering, College of Chemistry and Chemical Engineering, Shanghai University of Engineering Science, Shanghai 201620, People's Republic of China

Correspondence to: H. Wenli (E-mail: haowl1012@126.com)

**ABSTRACT:** The aim of this work was to study the effect of different organomontmorillonite on the structure and properties of room-temperature vulcanized silicone rubber (RTV) composites. Quaternary ammonium salts (QAS) and hyperbranched QAS were used as intercalation agents to treat Na<sup>+</sup>-montmorillonite and formed two kinds of organomontmorillonite, OMMT and HOMMT. OMMT/RTV and HOMMT/RTV composites were prepared using these organomodified silicate layers. Properties such as tensile strength, elongation at break, swelling behavior, and thermal stability were researched and compared. The addition of OMMT and HOMMT improved the mechanical properties of RTV composites. The composites with 3 mass % HOMMT showed the highest tensile strength and elongation at break, 5.4 MPa and 425%, which was 29 and 97% higher than that of pure RTV. The RTV composites exhibited excellent thermal stability and swelling behavior. At loading of 3 mass % of HOMMT,  $T_{\text{onset}}$  and  $T_{\text{max}}$  was 452 and 640°C, respectively, 33 and 150°C higher than that of pure RTV. A combination of X-ray diffraction (XRD) test, scanning electron microscopy (SEM), and transmission electron microscopy (TEM) studies was used to characterize the structure and reinforcing mechanism of these clays. The diffraction peaks in XRD curves were almost absent in the scattering curve of RTV/HOMMT (3 mass %). This was due to the possibility of having exfoliated silicate layers dispersed in the polymer matrix. A careful observation of an area of platelet tactoid of 3% HOMMT filled composite in SEM and TEM revealed the uniform dispersion of the silicate layers in the composites. © 2012 Wiley Periodicals, Inc. *J. Appl. Polym. Sci.* 129: 1852–1860, 2013

**KEYWORDS:** clay; thermal properties; rubber

Received 3 October 2012; accepted 30 November 2012; published online 24 December 2012

**DOI:** 10.1002/app.38887

### INTRODUCTION

Room-temperature vulcanized silicone rubber (RTV) is one of the most important types of high-temperature-resistant synthetic rubber with excellent thermal stability, low-temperature toughness, and electrical-insulating properties. It has been extensively used in electrical-insulating products, sealing products, and so forth. However, it is of low strength compared with that of other organic rubbers due to the weaker interaction between polysiloxane macromolecules.<sup>1</sup>

To meet the rising demands of applications, hybrids of inorganic “functional fillers” and polymeric materials were being continuously developed to combine their constituents’ beneficial properties or to induce new ones.<sup>2,3</sup> Montmorillonite (MMT), one of the layered clay minerals, is a type of hydrated aluminosilicate clay. The efficiency of MMT in improving the properties of polymeric materials is primarily determined by the degree of

its dispersion in the polymer matrix, which in turn depends on its particle size. However, the hydrophilic nature of the MMT surface impedes its homogeneous dispersion in the organic polymer phase.

To overcome this problem, making the surface organophilic prior to use is often necessary.<sup>4</sup> Some researchers prepared different types of intercalated silicate layers using different intercalation agents and examined their application properties in silicone rubber matrices. Mishra et al.<sup>5</sup> used quaternary long chain ammonium salt as an intercalation agent to treat MMT and improved its basal spacing. Silicone nanocomposites were prepared by solution blending with OMMT loading in the range of 2–10 mass %. The mechanical, thermal, and physical properties were improved compared to those of pristine silicone rubber due to OMMT exfoliation and uniform dispersion with good wet ability of the rubber chains. Zheng et al.<sup>6</sup> prepared

MMT/high-temperature silicone rubber hybrid nanocomposites via melt mixed process. Results proved that the nanocomposites with MMT treated with double octadecyl dimethyl ammonium chloride prepared by melt mixed could form intercalated structure. Furthermore, the mechanical property of the hybrids was improved. Jia et al.<sup>7</sup> incorporated five different types of OMMT into silicone rubber using a melt-blending method. Results revealed that the gas barrier property and the mechanical properties of the silicone rubber were obviously improved by the incorporation of 30 phr of OMMT. Wang et al.<sup>8,9</sup> prepared novel RTV/OMMT composites. Di(2-oxyethyl)-12 alkane-3 methyl-amine chloride and hydrogen silicone oil were used as intercalation agents to treat MMT and formed two kinds of OMMT. RTV/OMMT composites were prepared using these OMMT. Properties such as viscosity, hardness, tensile strength, elongation at break, and thermal stability were researched and compared. In addition, hyperbranched OMMT (HOMMT) was prepared by condensation reaction between OMMT and the monomer that we synthesized.<sup>10</sup> It was then used in the preparation of high-temperature vulcanized silicone rubber (HTV-SR)/HOMMT nanocomposite. Results showed that the tensile properties of HTV-SR/OMMT systems were better than that of the HTV-SR/OMMT and HTV-SR. This was probably due to the surface effect of the exfoliated silicate layers and anchor effect of HOMMT in the silicone rubber matrix. Rabova and Hron<sup>11</sup> evaluated the effect of surface-modified fillers based on MMT on rheological, mechanical properties, and thermal stability of high-molar mass polydimethylsiloxane matrix. Silicone rubber/clay composites were prepared via homogenization on open two roll-mill followed by torque measurement at two different temperatures. Synergism of fillers was also studied and led to an increase of tensile strength.

Most of these investigations emphasized the importance of the interlayer space of the clays using linear organic surfactants, which were not beneficial for the obvious improvement of interlayer space. This could result in no obvious improvement of thermal and other mechanical properties of the polymeric matrix.<sup>8</sup>

To overcome these problems, novel modification technology should be used. Recently, a new class of macromolecules, hyperbranched polymer has received more attention due to their special structures.<sup>12-14</sup> Hyperbranched polymers have a tree-like structure and plenty of functional end groups. This can make them more reactive. For high degree of branched structure, they are difficult to crystallize and have higher compatibility with other polymers.<sup>15</sup> In addition, hyperbranched polymers have better thermal stability than that of low molecular surfactant. Thus, it was expected that application of hyperbranched polymer will eventually lead to an improvement of thermal stability and compatibility for MMT with polymeric matrix.

In this study, organoclay reinforced RTV composites were prepared using quaternary ammonium salts (QAS) modified MMT (OMMT) and hyperbranched QAS (HQAS) modified MMT (HOMMT). These composites were prepared by solution intercalation. The composites with 3 mass % HOMMT showed the highest tensile strength and elongation at break, These RTV composites exhibited excellent thermal stability and swelling

behavior. X-ray diffraction (XRD) test, scanning electron microscopy (SEM), and transmission electron microscopy (TEM) studies were used to characterize the structure and reinforcing mechanism of these clays.

## EXPERIMENTAL

### Materials

Na<sup>+</sup>-MMT, industrial grade, was obtained from Zhejiang Fenghong Clay Company (Zhejiang, China). The inorganic MMT structural formula is Na<sub>0.71</sub>Ca<sub>0.06</sub>Mg<sub>0.014</sub>(Si<sub>7.80</sub>Al<sub>0.20</sub>)<sup>IV</sup>(Al<sub>3.14</sub>Fe<sup>3+</sup><sub>0.20</sub>Fe<sup>2+</sup><sub>0.04</sub>Mg<sub>0.62</sub>)<sup>VI</sup>O<sub>20</sub>(OH)<sub>4</sub>, and its cation exchange capacity is 90 cmol/kg. The formula indicates that the negative layer charge largely arises from isomorphous substitution of Mg<sup>2+</sup> for Al<sup>3+</sup> in the octahedral sheet (superscript VI) with some contribution from substitution of Al<sup>3+</sup> for Si<sup>4+</sup> in the tetrahedral sheet (superscript IV). The layer charge in MMT is dominantly balanced by Na<sup>+</sup> ions occupying interlayer sites. Di(2-oxyethyl)-12 alkane-3 methyl-amine chloride, denoted as QAS, chemical pure, was received from Zhejiang Chemical Agent Company (Zhejiang, China). HQAS, denoted as HQAS, was synthesized by us.<sup>16</sup> The structures of these two surfactants are shown in Figure 1(a,b).

RTV, two components (A : B, 1 : 1, 30% aerosilica, component A: hydrogenous silicane, Si-(O-Si-(CH<sub>3</sub>)<sub>2</sub>-H)<sub>4</sub>; component B: ethylene-terminated polysiloxane, CH<sub>2</sub>=CH-Si(CH<sub>3</sub>)<sub>2</sub>O(Si(CH<sub>3</sub>)<sub>2</sub>O)<sub>n</sub>-Si(CH<sub>3</sub>)<sub>2</sub>-CH=CH<sub>2</sub>, and the organic platinum catalyst), industrial grade, were supplied by Bluestar Silicones Shanghai Company (Shanghai, China).

### Modification of Na<sup>+</sup>-MMT

The QAS- and HQAS-modified MMTs were prepared by cation exchange as reported before.<sup>16</sup> Ten grams of MMT was gradually added to a prior prepared solution of QAS (3.52 g) or HQAS

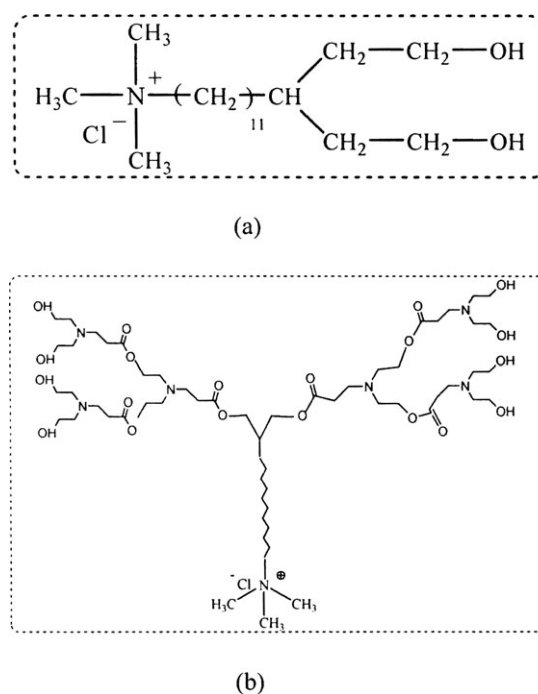


Figure 1. Structure of organic surfactants: (a) QAS and (b) HQAS.

(5 g), which were dissolved of 120 mL of ethanol and water mixture (weight ratio, 1 : 1). The resultant suspension was vigorously stirred for 2 h. The treated MMT was repeatedly washed by deionized water. The filtrate was titrated with 0.1 N of AgNO<sub>3</sub>, until no precipitate of AgCl was formed to ensure the complete removal of chloride ions. The filter cake was then placed in a vacuum oven at 80°C for 12 h for drying. The obtained organomontmorillonites were denoted as OMMT and HOMMT.

### Preparation of RTV Composites

Different amounts of OMMT or HOMMT (1, 3, 5, 7, and 9 mass %) were mixed with 10 g of hydrogenous silicane, one component of RTV. After vigorous stirring at room temperature for 3 h (high-speed stirring machine, U400, 4000–6000 rpm, Shanghai Modern Environmental Engineering Technology, Shanghai, China), the mixture was blended with 10 g of ethylene-terminated polysiloxane, the other component of RTV, and stirred for 30 s. Then, the mixture was molded in a Teflon mold. Curing was conducted at room temperature, 20°C, for 24 h, after which different elastic films were obtained.

### Characterization

The tensile properties of the vulcanizates were measured with dumbbell specimens (6-mm wide in cross section) according to the Chinese National Standard GB 528-82. Tensile test was carried out using a TCR-2000 instrument (Gaotie Company, Taiwan, China) at room temperature with a crosshead speed of 500 mm/min. The samples were manufactured in a standard dumbbell shape with 1.8–2.2 mm in thickness, and all measurements were repeated five times, and medium data were obtained.

Swelling test was conducted by using vulcanized 5.0 × 2.5 × 0.2 cm<sup>3</sup> samples. They were weighed and allowed to swell in an excess of toluene at room temperature, in the dark, until equilibrium was achieved. The swollen samples were then weighed, and the solvent removed under vacuum and weighed again. The volume fraction of the rubber in the swollen vulcanizates ( $V_r$ ) was calculated using the following equation:<sup>17</sup>

$$V_r = \frac{(m_1/\rho_r) - V_f}{(m_1/\rho_r) - V_f + (m_2 - m_3)/\rho_s}$$

where  $m_1$  is the initial weight of specimen,  $m_2$  is the weight of swollen specimen,  $m_3$  is the weight of specimen after equilibrium,  $V_f$  is the volume of filler,  $\rho_r$  is the density of rubber, and  $\rho_s$  is the density of solvent (0.8669 for toluene).  $V_r$  was substituted in the Flory–Rehner equation as follows:

$$v = \frac{\ln(1 - V_r) + V_r + \mu V_r^2}{V_0(V_r^{1/3} - V_r/2)}$$

where  $v$  is the cross-linking density,  $V_r$  is the volume fraction of the rubber in the swollen vulcanizates,  $\mu$  is the parameter characteristic of interaction between the rubber network and the swelling agent, and  $V_0$  is the molar volume of toluene ( $V_0 = 106.2$  cm<sup>3</sup>/mol). The polymer–solvent interaction parameter used was about 0.4.<sup>18</sup>

Thermogravimetric analysis (TGA) were carried out at 10°C/min under air (flow rate  $5 \times 10^{-7}$  m<sup>3</sup>/s, air liquid grade) using a Linseis PT-1000 equipment (Linseis Company, Selb, Germany). In each case, the mass of the sample used was fixed at 10 mg, and the samples (powder mixtures) were positioned in open vitreous silica pans. The precision of the temperature measurements was 1°C over the whole range of temperatures. The heat of fusion and glass transition temperature were obtained with a Linseis PT-10 equipment (Linseis Company).

To measure the change of gallery distance before and after intercalation, XRD was performed at room temperature with a Rigaku D-Max/400 (Rigaku Company, Akishima, Japan) X-ray diffractometer. The X-ray beam was nickel-filtered CuK $\alpha$  ( $\lambda = 0.154$  nm) radiation operated at 50 kV and 150 mA. XRD data were obtained from 1 to 10° ( $2\theta$ ) at a rate of 2°/min.

SEM was carried out using Hitachi S-2150 instrument at a voltage of 30 kV (Hitachi, Tokyo, Japan). The samples were gold coated using an IB-3 Ionic sputtermeter.

TEM observation was performed on ultrathin films prepared by cryoultramicrotomy using a JEM-2010 instrument (JEOL, Tokyo, Japan) at an acceleration voltage of 80 kV. The thin sections were sliced with a microtome into 80–100 nm thickness at –100°C.

## RESULTS AND DISCUSSION

### The Effect of OMMT and HOMMT on Tensile Properties of RTV Composites

The tensile strength and elongation at break of different RTV composites were increased with the amount of clays, when their contents were <3 mass % (Figure 2). The HOMMT and OMMT reinforced RTV showed better tensile properties than that of MMT filled composites. At 3 mass %, the RTV/HOMMT composites showed the highest tensile strength, 5.4 MPa, which was 29% higher than that of pure RTV. Highest elongation at break was 425%, which was 97% higher than that of pure RTV. The improvement of tensile properties was attributed to two facts: (1) uniformly dispersed HOMMT with low aspect ratio possessed a higher stress bearing capability and efficiency and (2) stronger interactions between HOMMT and RTV chains associated with the larger contact surface and more active sites, which might induce differentiated curing efficiency and result in more effective constraint of the motion of rubber chains. The mechanism of RTV/HOMMT (3 mass %) was assumed to be chain slippage and “zig-zag” energy dissipation (Figure 3).<sup>19</sup> The silicate layers dispersed almost uniformly in the polymeric matrix, like various pine needles. The reaction between the hydroxyl groups in HOMMT and molecular chains in RTV can improve the crosslinking degree of this matrix and, thus, can restrict the movement of polymer chains and combine them with silicate layers.

The crack path around the silicate layers could be considered as a mechanism of energy dissipation. By this suggested model, the increase in tensile properties seemed to be as expected for this reinforced composite.<sup>20,21</sup> Further addition of these clays decreased the tensile properties. As their contents were increased, some silicate layers aggregated.<sup>22</sup> The formation of

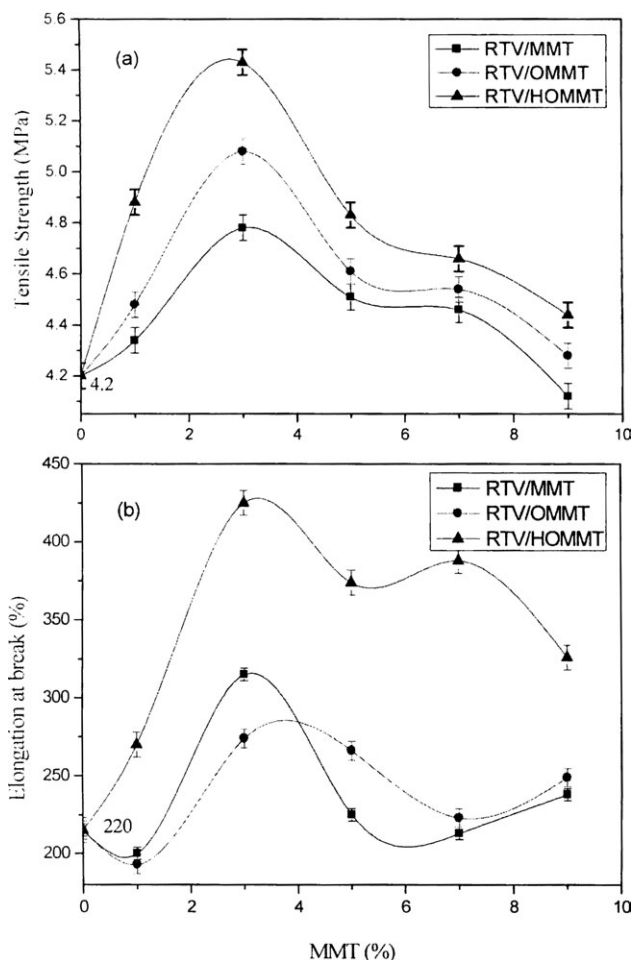


Figure 2. Tensile properties of RTV composites: (a) tensile strength and (b) elongation at break.

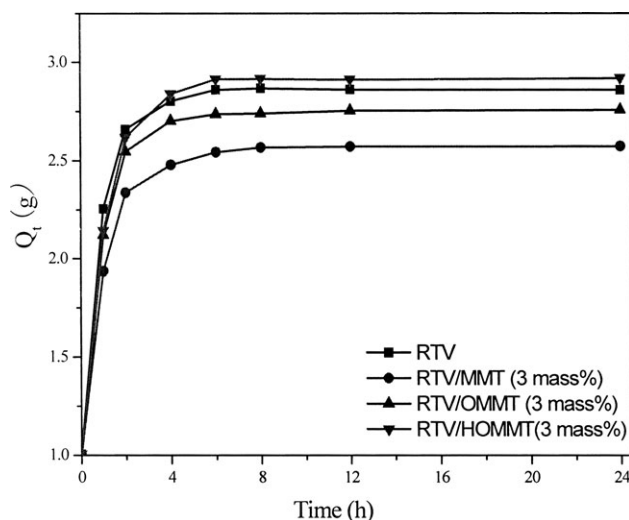


Figure 4. Swelling behavior of RTV composites in toluene at 25°C.

clay aggregates reduced the interface area between polymer and the silicate layers, which decreased the mechanical properties.

#### The Effect of OMMT and HOMMT on Swelling Behavior of RTV Composites

The swelling test had some relationship with the tensile properties of RTV composites. The original RTV, RTV/OMMT, and RTV/HOMMT (3 mass %) had the obvious solvent adsorption behavior, whereas RTV/MMT (3 mass %) had the lowest (Figure 4). The more the networks, the more was the absorption capacity of solvent.<sup>23,24</sup> This could illustrate that more networks existed in OMMT and HOMMT reinforced composites due to good dispersion of silicate layers and the strong interactions between silicate layers and RTV matrix. Table I shows the

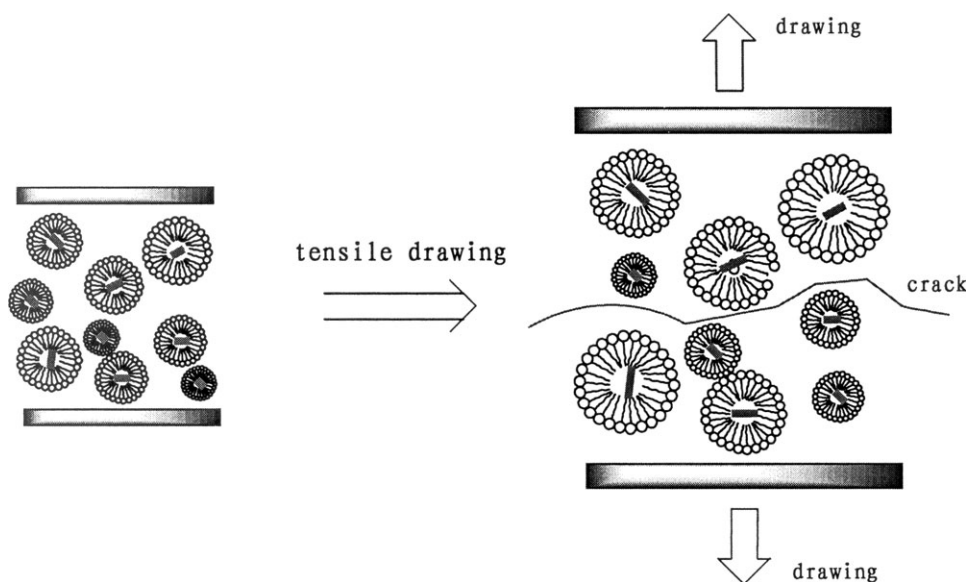


Figure 3. Scheme of tensile drawing process of RTV/HOMMT (3 wt. %) composites.



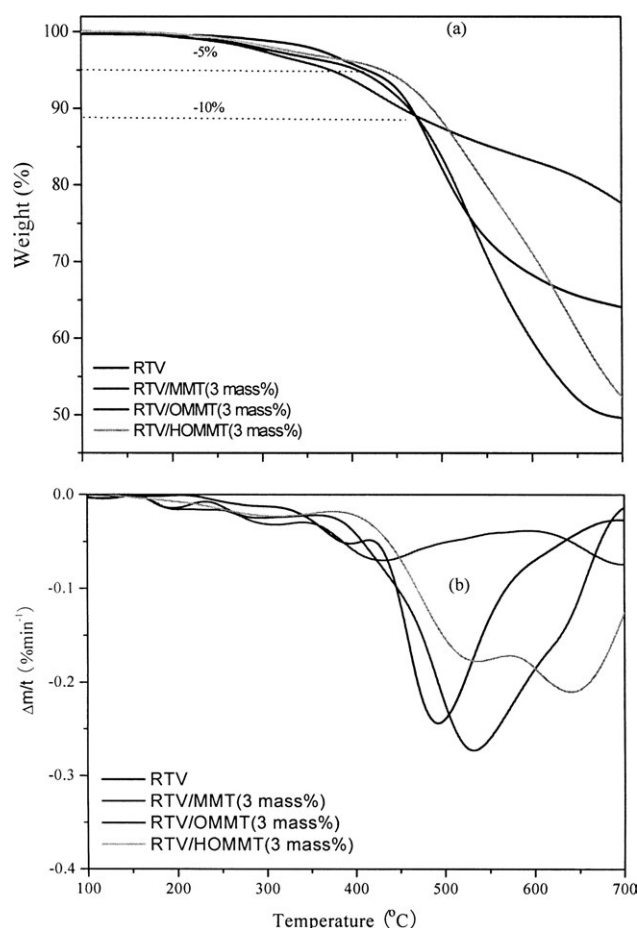
**Table I.** Crosslinking Densities of Different RTV Composites

	$\nu$
RTV	7.27
RTV/Na <sup>+</sup> -MMT (3 mass %)	6.44
RTV/OMMT (3 mass %)	7.41
RTV/HOMMT (3 mass %)	9.87

variation of crosslinking density  $\nu$  for each composition.<sup>25</sup> In the composition with MMT, the crosslinking density was decreased with the addition of 3 phr of MMT. This was attributed to the increasing damage of networks by the increasing amount of fillers. The addition of 3 phr of OMMT and HOMMT increased the crosslinking density of RTV, and this was in good agreement with their tensile properties. Generally speaking, appropriate amount of HOMMT had a positive effect on the development of crosslinking networks in the RTV matrix.

### The Effect of OMMT and HOMMT on Thermal Properties of RTV Composites

To compare their thermal stabilities clearly, three parameters were measured from the TGA and DTG curves (Figure 5), that is, the onset temperature of thermal degradation ( $T_{\text{onset}}$ , the temperature at which weight loss is 5 mass %), the center

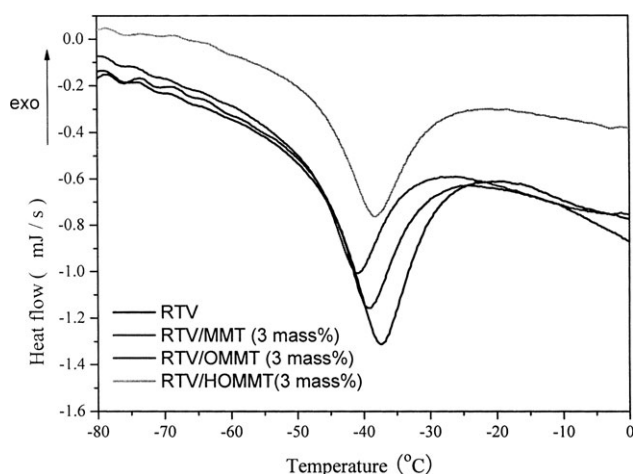
**Figure 5.** Thermal stability of RTV composites: (a) TGA and (b) DTG.**Table II.** TGA Results for the Thermal Degradation of Different RTV Composites

	$T_{\text{onset}}$ (°C)	$T_{\text{max}}$ (°C)	Residual mass (%)
RTV	419	490	64.2
RTV/Na <sup>+</sup> -MMT (3 mass %)	398	695	77.8
RTV/OMMT (3 mass %)	412	530	51.5
RTV/HOMMT (3 mass %)	452	640	53.2

temperature of thermal degradation ( $T_{\text{max}}$ , the temperature at which weight loss is the fastest), and the yield of charred residue at 700°C.<sup>26</sup>

Overall, the thermal stability of RTV/HOMMT composites was better than that of RTV/OMMT (Table II). The  $T_{\text{onset}}$  and  $T_{\text{max}}$  of the composites RTV/HOMMT were higher than those of RTV/OMMT. At loading of 3 mass % of HOMMT,  $T_{\text{onset}}$  and  $T_{\text{max}}$  was 452 and 640°C, respectively, 40 and 110°C higher than that of 3 mass % of OMMT reinforced composite. This was due to the improvement of thermal stability of the ammonium salt caused by the hyperbranched polymer chains. The well-dispersed silicate layers not only hindered the evaporation of decomposition products but also more effectively hindered the access of oxygen to the polymer, reducing the rate of initiation of polymer chain scission to produce volatile small products. The high decomposition temperature indicated the improved thermal stability of the composites. However, it is not so obvious that the nanocomposites delivered the best thermal stability. For example, the RTV according to Figure 5 had higher onset temperature than RTV/OMMT, and the lowest rate of weight loss was presented by RTV/MMT. This was mainly attributed to the higher ratio of inorganic silicate layers presented in MMT. These inorganic silicate layers had higher thermal stability compared with that of organic silicate layers both in OMMT and in HOMMT.

A transition of RTV existed at  $-37.5^{\circ}\text{C}$ , corresponding to the glass-to-rubber transition temperature ( $T_g$ ) of pure RTV (Figure 6). With the addition of MMT and OMMT to system,

**Figure 6.** DSC curves of RTV composites.

the glass transition temperatures of RTV/MMT and RTV/OMMT composites decreased about 5 and 2.5°C, respectively. In the present case, the introduction of silicate layers could introduce free volume and lead to the incomplete curing reaction in these composites and thus might decrease the system's  $T_g$ .

However, after modification by hyperbranched technology, the addition of silicate layers increased  $T_g$  from  $-42.5$  to  $-38^\circ\text{C}$ . These could be caused by at least following two reasons. First, the nanoreinforcement effect of HOMMT layers, which were dispersed in the continuous RTV matrix and restricted the motion of polymer chains, may give rise to the increase in  $T_g$ . Second, the hyperbranched polymers had the effect of reinforcement on polymer networks, which could also lead to the rise of  $T_g$ .<sup>27,28</sup>

### The Effect of OMMT and HOMMT on Microstructure of RTV Composites

The original MMT showed a (0 0 1) reflection at  $2\theta = 5.8^\circ$ , corresponding to the basal spacing of 1.5 nm. After organic modification with QAS, the basal spacing was increased to 1.6, 2.5, and 4.9 nm. The basal spacings of 2.5 nm for HOMMT were consistent with bilayer to pseudotrilyer arrangement of intercalated surfactants (Figure 7).

Nearly no peaks were observed indicating the original microstructure of RTV (Figure 8). When a small amount (3 mass %) of MMT and OMMT was incorporated, only very slight peaks appeared. These peaks corresponded to the d-spacing of MMT and OMMT. This phenomenon illustrated the existence of stacked silicate layers in these composites.<sup>29,30</sup> The diffraction peaks (curve (c)) were almost absent in the scattering curve of RTV/HOMMT (3 mass %). This was probably ascribed to the loss of structure registry, indicating the possibility of having exfoliated silicate layers dispersed in the polymer matrix.

### The Effect of OMMT and HOMMT on Morphology of RTV Composites

To further explain this phenomenon observed from XRD patterns, the morphological structures of relevant samples were analyzed by SEM and TEM.

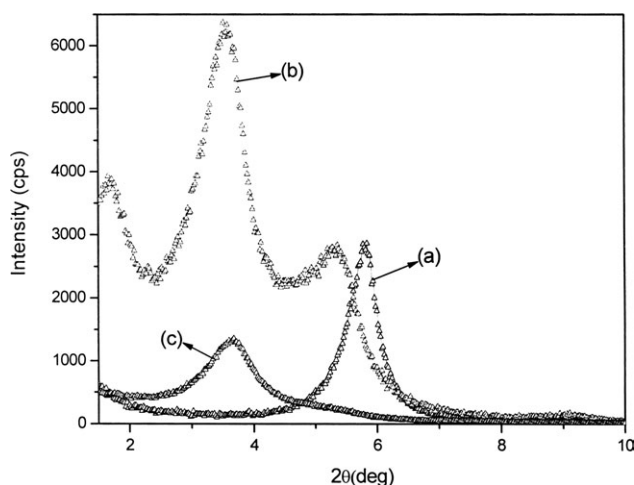


**Figure 7.** XRD curves of (a) MMT, (b) QAS-OMMT, and (c) HQAS-OMMT.

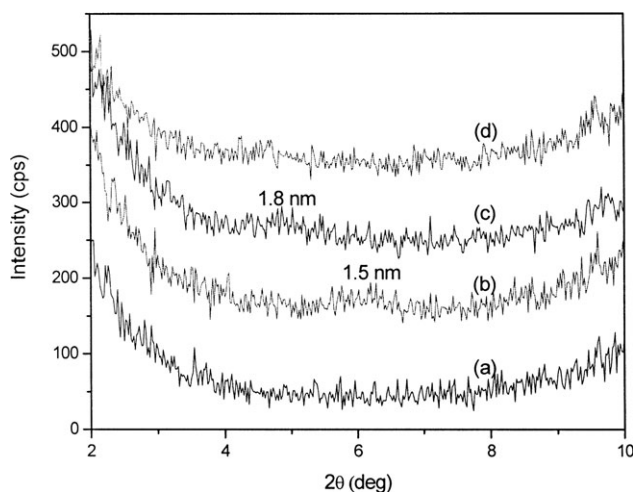


**Figure 8.** XRD curves of (a) RTV, (b) RTV/ $\text{Na}^+$ -MMT (3 mass %), (c) RTV/OMMT (3 mass %), and (d) RTV/HOMMT (3 mass %).

Original MMT layers were irregularly dispersed on the surface of RTV matrix and formed holes and agglomerates [Figure 9(a)]. Compared with RTV/MMT system, the RTV/OMMT system formed almost scattered powder morphology [Figure 9(b)]. Although this morphology was almost the same, with the addition of HOMMT, the regularly scattered dispersion of HOMMT layers was still observed [Figure 9(c)].

Further evidence of nanometer-scale dispersion of silicate layers in the case of different RTV composites was supported by TEM photomicrographs (Figure 10). The MMT layers did not fill the full volume, suggesting that the platelet tactoids of MMT were dispersed in RTV matrix at aggregated scales [Figure 10(a)]. Exfoliated clay layers could be observed for both RTV/OMMT [Figure 10(b)] and RTV/HOMMT [Figure 10(c)] vulcanizates. Additionally, their XRD spectra are quite similar (at 1.8 nm). A close observation of an area of platelet tactoid of 3% HOMMT filled composite revealed the individual platelets of HOMMT clearly separated by polymer matrix, that is, some polymer had diffused between some of the platelets. The dark zones were the cross-sections of the silicate layers. The silicate layers were parallel to the surface of the films and were dispersed in the RTV matrix. This was evidence that these organoclays were mostly exfoliated in the RTV matrix.<sup>31</sup> The formation of exfoliated clay composites was dependent on the nature of the intercalation agents, and the ammonium with long chains could allow more organic species to diffuse into the layered silicates.<sup>32</sup> The subsequent polymerization could be a driving force between the negatively charged silicate layers and the gallery cations.

### CONCLUSIONS

RTV/OMMT and RTV/HOMMT composites were prepared by solution intercalation. XRD and TEM analysis indicated that the RTV chains were intercalated for OMMT and were almost exfoliated for HOMMT.

The introduction of OMMT and HOMMT improved the mechanical properties of RTV composites. The composites with 3 mass % HOMMT showed the highest tensile strength and



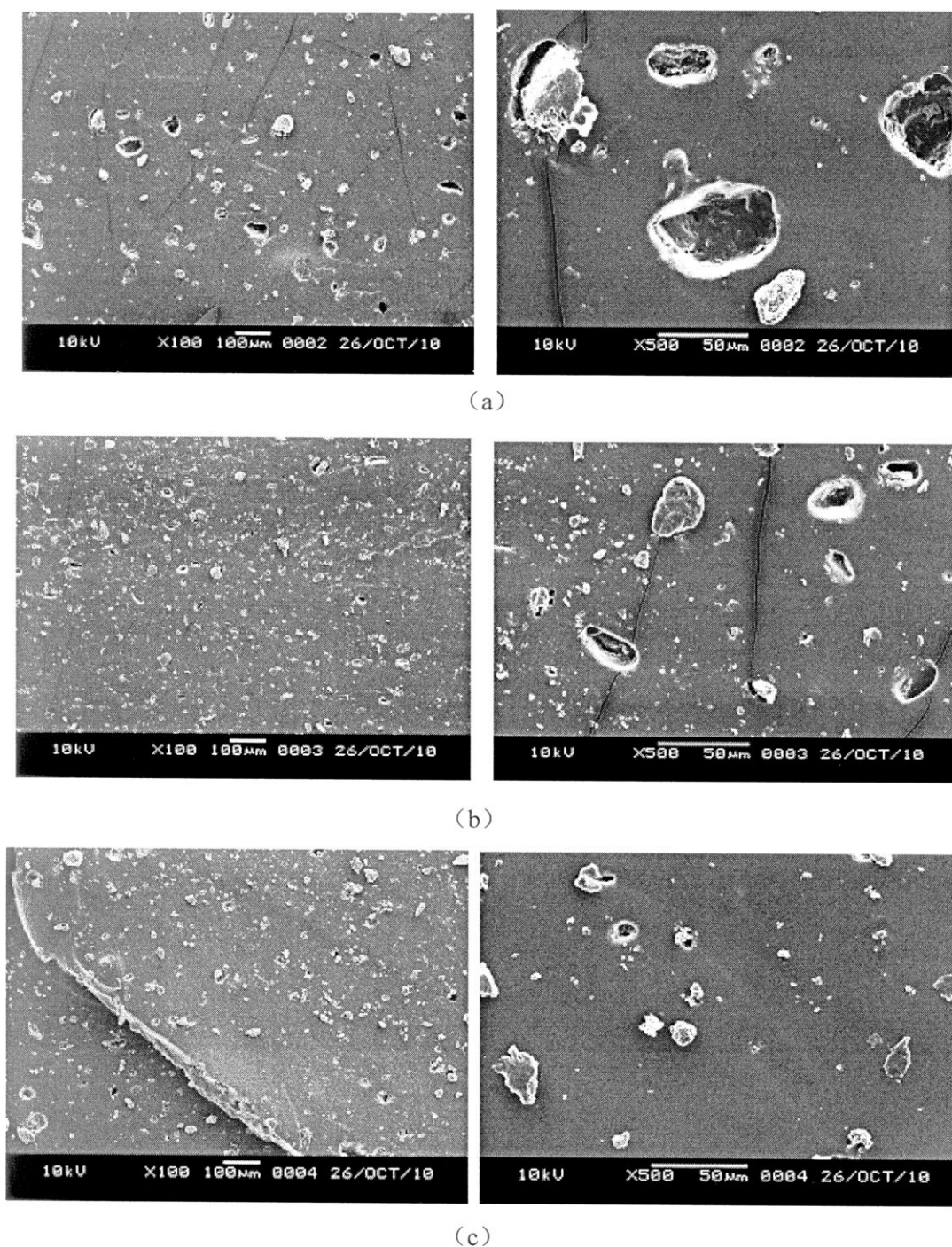


**Figure 9.** SEM images of (a) RTV/Na<sup>+</sup>-MMT (3 mass %), (b) RTV/OMMT(3 mass %), and (c) RTV/HOMMT (3 mass %).

elongation at break, 5.4 MPa and 425%, which was 29 and 97% higher than that of pure RTV.

The RTV composites with HOMMT exhibited better thermal stability and higher crosslinking degree than that of OMMT reinforced ones. This was attributed to the uniform dispersion and stronger interactions of the silicate layers in the composites.

#### ACKNOWLEDGMENTS

This work was financially supported by “National Natural Science Funds (Project Nos. 50803034 and 51173102),” “Shu Guang’ project (Project No. 10SG53) supported by Shanghai Municipal Education Commission and Shanghai Education Development Foundation,” “Shanghai Talent Development Fund (Project (2012) No. 23),” “Shanghai Universities Knowledge Innovation



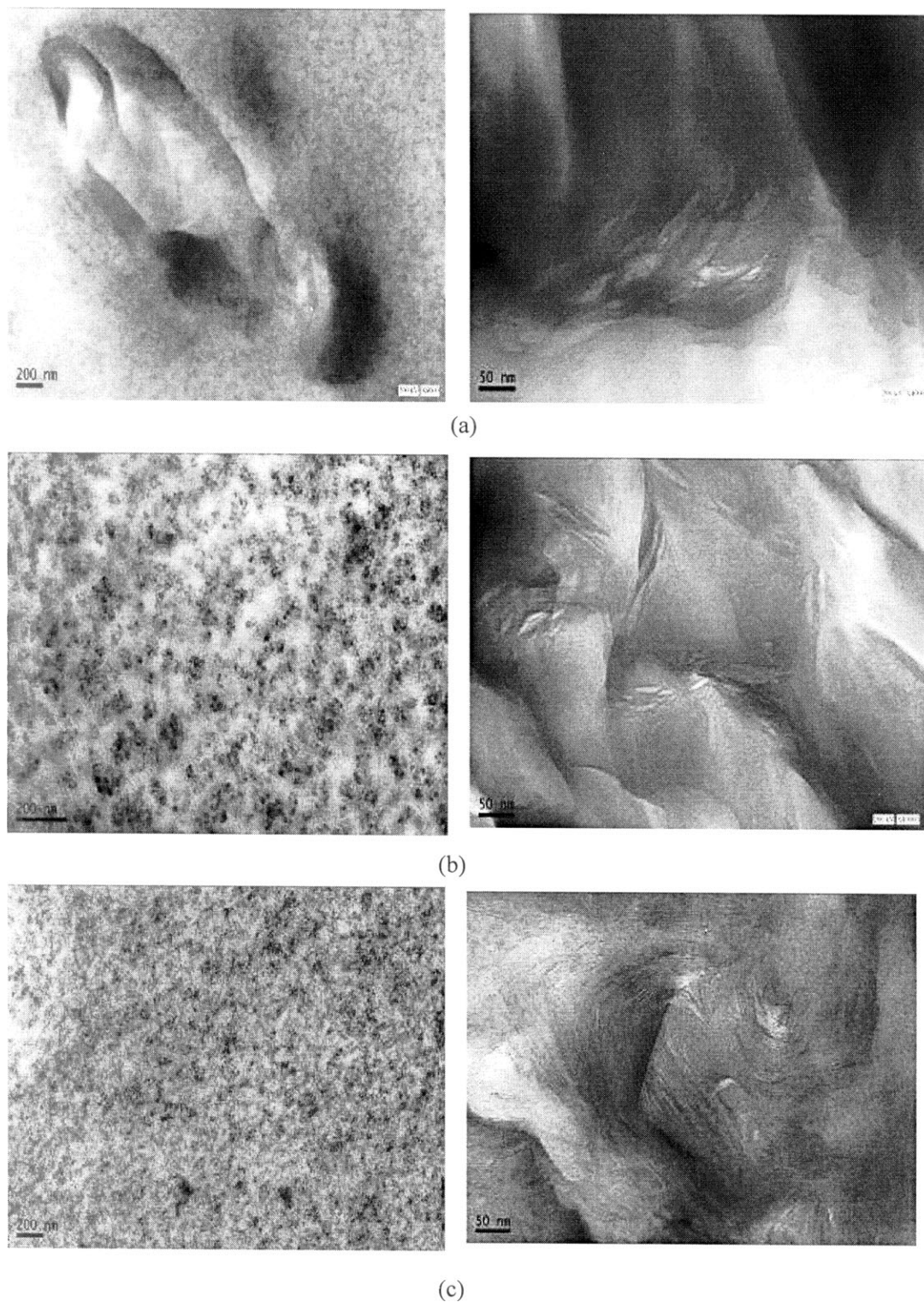


**Figure 10.** TEM images of (a) RTV/Na<sup>+</sup>-MMT (3 mass %), (b) RTV/OMMT(3 mass %), and (c) RTV/HOMMT (3 mass %).

Engineering Project (Project No. JZ0904),” “Construction of Innovative Team on Natural source of pharmaceutical engineering Project (Project No. XKCZ1205),” “Capacity-building of Local University Project by Science and Technology Commission

of Shanghai Municipality (Project No. 11490501500),” and “Students Research and Training Project of Shanghai University of Engineering Science (Project Nos. 2012xs57, cx1204001, and cs1204007).



## REFERENCES

1. Wang, J. C.; Chen, Y. H.; Jin, Q. Q. *Macromol. Chem. Phys.* **2005**, *206*, 2512.
2. Sepulcre-Guilabert, J.; Ferrandiz-Gomez, T. P.; Martin-Martinez, J. M. *J. Adhes. Sci. Technol.* **2001**, *15*, 187.
3. Ma, J.; Xu, J.; Ren, J. H.; Yu, Z. Z.; Mai, Y. W. *Polymer* **2003**, *44*, 4619.
4. Xi, Y.; Frost, R. L.; He, H.; Kloprogge, T.; Bostrom, T. *Langmuir* **2005**, *21*, 8675.
5. Mishra, S.; Shimpi, N.; Mali, A. D. *Macromol. Res.* **2012**, *1*, 1.
6. Zheng, J. P.; Zhang, W.; Li, H. Y.; Li, J. J. *Polym. Res.* **2011**, *18*, 2359.
7. Jia, C.; Zhang, L. Q.; Zhang, H.; Lu, Y. L. *Polym. Compos.* **2011**, *32*, 1245.
8. Wang, J. C.; Yang, K.; Xu, N. *J. Appl. Polym. Sci.* **2012**, *123*, 1293.
9. Wang, J. C.; Chen, Y. H.; Jin, Q. Q. *High Perform. Polym.* **2006**, *18*, 325.
10. Wang, J. C.; Chen, Y. H.; Wang, J. H. *J. Appl. Polym. Sci.* **2009**, *111*, 658.
11. Rabova, V.; Hron, P. *E-Polymers* **2011**, A91.
12. Wang, J. C.; Guo, X.; Zheng, X. Y.; Zhao, Y.; Li, W. F. *Clays Clay Miner.* **2011**, *59*, 446.
13. Tan, H. M.; Luo, Y. J. *Hyper-Branched Polymers*; Chemical Industry Press:Beijing, **2005**.
14. Gao, C.; Yan, D. Y. *Prog. Polym. Sci.* **2004**, *29*, 183.
15. Marlene, R.; Christopher, J. G. P.; Laszlo, G.; Yves, L.; Henri, J. M. G.; Jan-Anders, E. M. *Polymer* **2004**, *45*, 949.
16. Wang, J. C.; Zheng, X. Y.; Hao, W. L.; Xu, N.; Pan, X. C. *Powder Technol.* **2012**, *221*, 80.
17. Daniele, F. C.; Joao Carlos, M. S.; Regina, C. R. N.; Leila, L. Y. V. *J. Appl. Polym. Sci.* **2003**, *90*, 2156.
18. Lide, D. R. *Handbook of Chemistry and Physics*, 76th ed.; CRC Press: Boca Raton, **1995**.
19. Gatos, K. G.; Sawanis, N. S.; Apostolov, A. A.; Thomann, R.; Karger-Kocsis, J. *Macromol. Mater. Eng.* **2004**, *289*, 1079.
20. Kojima, Y.; Usuki, A.; Kawasumi, M. *J. Mater. Res.* **1993**, *6*, 1185.
21. Gu, Z.; Song, G. J.; Liu, W. S.; Wang, B. J.; Li, J. *Appl. Clay Sci.* **2009**, *45*, 50.
22. Shi, X. D.; Gan, Z. H. *Eur. Polym. J.* **2008**, *43*, 4852.
23. Jia, D. M.; Li, Y. M. *J. Appl. Polym. Sci.* **2000**, *78*, 2482.
24. Gu, Y. Y.; Zheng, Q. Y.; Ye, L. *China Plast. Ind.* **2007**, *35*, 127.
25. He, G.; Chen, Y.; Zhang, M. M.; Wang, D. X.; Cong, K.; Fan, H. B.; Zhou, F. J. *Polym. Mater. Sci. Eng.* **2011**, *27*, 150.
26. Xia, Y.; Jian, X. G.; Li, J. F.; Wang, X. H.; Xu, Y. Y. *Polym.-Plast. Technol. Eng.* **2007**, *46*, 227.
27. Wang, J. C.; Zheng, X. Y.; Hao, W. L.; Zhao, Y. *Elastomers* **2012**, *22*, 59.
28. Zanetti, M.; Camino, G.; Reichert, P. *Macromol. Rapid Commun.* **2001**, *22*, 176.
29. Wang, J. C.; Chen, Y. H.; Chen, R. J. *J. Polym. Sci. Part B: Polym. Phys.* **2007**, *45*, 519.
30. Lan, T.; Kaviratan, P. D.; Pinnavaia, T. J. *Chem. Mater.* **1995**, *7*, 2144.
31. Mousa, A.; Karger-Kocsis, J. *Macromol. Mater. Eng.* **2001**, *286*, 260.
32. Yoon, K. B.; Sung, H. D.; Hwang, Y. Y.; Noh, S. K.; Lee, D. H. *Appl. Clay Sci.* **2007**, *38*, 1.